Odd aberrations and double-pass measurements of retinal image quality

Pablo Artal

Laboratorio de Optica, Departamento de Física, Universidad de Murcia, Campus de Espinardo, 30071 Murcia, Spain

Susana Marcos and Rafael Navarro

Instituto de Optica, Consejo Superior de Investigaciones Científicas, Serrano 121, 28006 Madrid, Spain

David R. Williams

Center for Visual Sciences, University of Rochester, Rochester, New York 14627

Received January 25, 1994; revised manuscript received July 21, 1994; accepted September 6, 1994

We investigated the formation of the aerial image in the double-pass method to measure the optical quality of the human eye. We show theoretically and empirically that the double pass through the eye's optics forces the light distribution in the aerial image to be an even-symmetric function even if the single-pass point-spread function is asymmetric as a result of odd aberrations in the eye. The reason for this is that the double-pass imaging process is described by the autocorrelation rather than the autoconvolution of the single-pass point-spread functions, as has been previously assumed. This implies that although the modulation transfer function can be computed from the double-pass aerial image, the phase transfer function cannot. We also show that the lateral chromatic aberration of the eye cannot be measured with the double-pass procedure because it is canceled by the second pass through the eye's optics.

1. INTRODUCTION

The double-pass method (or ophthalmoscopic technique) has been widely used to measure retinal image quality in the human eye (see, for instance, Ref. 1 for a recent general review). When an object is imaged onto the retina, a fraction of the light is reflected back and the external retinal image (aerial image) is used to estimate the aberrations of the eye, the point-spread function (PSF), the line-spread function, and the ocular modulation transfer function (MTF). Flamant[2] obtained the first double-pass line-spread function recorded photographically, and later other authors used photomultipliers to scan the aerial image of lines, edges, and gratings.[3–7] More recently we developed an improved version of the double-pass system, recording the aerial image of a point source with electronic imaging devices such as CCD arrays.[8,9]

The double-pass method offers several advantages over other methods for estimating retinal image quality. It is an objective method that is comfortable for the subject. It takes less than 10 min to obtain a complete two-dimensional MTF with our experimental system.[8,9] It is also applicable to the peripheral retina,[10] where neural limitations make it difficult to apply subjective methods. However, the technique also has its limitations. One involves uncertainties about how the reflection of light from different retinal layers affects the estimate of the MTF. Van Blockland and van Norren[11] observed two components in the retinal reflection, a wide scattering halo and a specular component, and Gorrand[12] concluded from his experiments that the double-pass method should underestimate the image quality of the eye. However, by recording the retinal image of two points simultaneously, we showed[9] that the retina in the central fovea has little effect on the double-pass MTF. In addition, Williams *et al.*[13] recently compared the MTF's obtained with double-pass and psychophysical methods. They showed that although the double pass tends to underestimate the MTF slightly, especially for high spatial frequencies, most of the light that forms the double-pass image seems to come from the entrance aperture of photoreceptors and not from other retinal layers. Another difficulty with the double-pass method is that the field of view over which the aerial image is collected can affect the MTF estimate.[14] One approach to this problem is to estimate the PSF over a wide angle by combining double-pass with psychophysical glare measurements.[15] Alternatively, on can capture a large fraction of the aerial image with a CCD array that permits accurate absolute radiometric measurements of the aerial image tails.[13] So despite the problems of interpreting the aerial image, it is clear that the double-pass image available outside the eye is well correlated with the single-pass light distribution on the retina.

On the other hand, the estimates of some ocular aberrations obtained from double-pass measurements are different from those obtained with subjective methods.[16,17] Large amounts of comalike aberrations were found with the subjective methods, whereas the double-pass results do not show significant values of odd aberrations either in the fovea or in the periphery. Moreover, when we recently used the double-pass method to measure retinal image quality with decentered artificial pupils,[18] which should have produced coma, the aerial images were even

0740-3232/95/020195-07$06.00　

symmetric. These facts suggested that the double-pass configuration might produce only even aerial images. In this paper we show that the double-pass method loses the phase of the optical transfer function and estimates of odd aberrations, such as coma or distortion. However, we also show that this loss of phase does not influence the correct estimation of the eye's MTF.

2. IMAGE FORMATION IN THE DOUBLE-PASS METHOD

A. Theory

Figure 1 shows a schematic diagram of the image-formation process for an off-axis point test in a system with comalike aberrations (odd wave aberration). In the figure, x, y are spatial coordinates in the object plane; x', y' are spatial coordinates in the single-pass plane (the retina in the case of the eye); x'', y'' are spatial coordinates in the second-pass plane (aerial image); d, d' are the object and the image distance, respectively, and the refractive index has been assumed to be unity in the object and image space for the sake of clarity. This figure mimics the situation in the eye, where if we assume that the eye is a reversible optical system and is locally isoplanatic in the fovea,[9] the whole process can be unfolded in two equivalent stages (first and second passages) having approximately the same optical performance. The amplitude-spread function for the first pass between planes (x, y) and (x', y') can be written as[19]

$$h(x', y'; x, y) = \frac{1}{\lambda^2 dd'} \iint \exp[iW(\xi_1, \eta_1)] \times \exp\left\{-i\frac{2\pi}{\lambda d'}[(x' + mx)\xi_1 + (y' + my)\eta_1]\right\} d\xi_1 d\eta_1 = h_1(x' + mx, y' + my), \quad (1)$$

where ξ_1, η_1 are the pupil plane coordinates and λ the wavelength of the incident light. The wave aberration at the pupil exit, $[W(\xi_1, \eta_1)]$, is measured as the phase difference between the ideal spherical wave front and the real wave front of the system. The magnification of the system is negative, and in Eq. (1), m represents the modulus of the magnification ($m = |d'/d|$). The integration is performed in the pupil area, and the phase quadratic factors are not included in Eq. (1) and the following equations for simplicity. The amplitude response for the second pass between planes (x', y') and (x'', y'') is

$$h(x'', y''; x', y') = \frac{1}{\lambda^2 dd'} \iint \exp[-iW(\xi_2, \eta_2)] \times \exp\left\{-i\frac{2\pi}{\lambda d}\left[\left(x'' + \frac{1}{m}x'\right)\xi_2 + \left(y'' + \frac{1}{m}y\right)\eta_2\right]\right\} d\xi_2 d\eta_2 = h_2{}^*\left(x'' + \frac{1}{m}x', y'' + \frac{1}{m}y'\right), \quad (2)$$

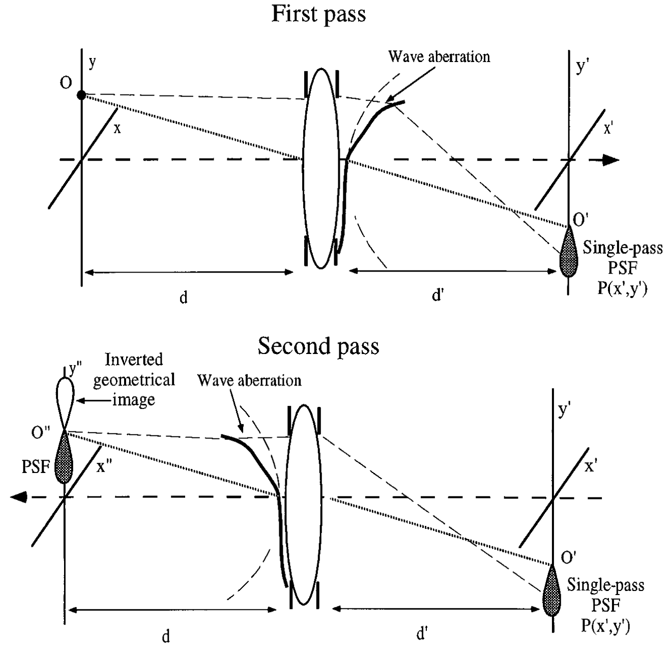

Fig. 1. Schematic diagram of the image-formation process in the double pass. x, y, object coordinates; x', y', image-plane (retinal) coordinates; x'', y'', double-pass coordinates; d, d', object and image distances, respectively. Object O is a point test, and $P(x', y')$ is the single-pass PSF.

where ξ_2, η_2 are coordinates at the second-pass exit-pupil plane and the asterisk denotes complex conjugation. In the paraxial approximation (assuming small aberrations), the wave aberration will be the same in both passages, except for a change of sign (as is shown in Fig. 1). Taking into account that $d' = -dm$ (with the sign convention, d negative and d' positive), Eqs. (1) and (2) are formally equal, having the following relationship:

$$h_1(x' + mx, y' + my) = h_2{}^*\left(x + \frac{1}{m}x', y + \frac{1}{m}y'\right) \cdot \quad (3)$$

The amplitude distribution of a point source {expressed by a Dirac delta function, $[O(x, y) = \delta(x, y)]$} in the first pass is $h_1(x', y')$, and after reflection in the retina and the second pass through the eye the amplitude distribution of the aerial image $[O_i''(x'', y'')]$ is given by the superposition integral[19]

$$O_i''(x'', y'') = \iint \left[h_2{}^*\left(x'' + \frac{1}{m}x', y'' + \frac{1}{m}y'\right)\right] \times [h_1(x', y')R_i(x', y')]dx'dy', \quad (4)$$

where R_i is the amplitude reflection factor in the retina. With an additional change of variable $[\bar{x}' = -(1/m)x', \bar{y}' = -(1/m)y']$ and using the relationship of Eq. (3), we can rewrite Eq. (4) as

$$O_i''(x'', y'') = m^2 \iint h_1(mx'' - m\bar{x}', my'' - m\bar{y}') \times [h_1(-m\bar{x}', -m\bar{y}')R_i(-m\bar{x}', -m\bar{y}')]d\bar{x}'d\bar{y}' = m^2[h_1(mx'', my'')] \otimes [h_1(-mx'', -my'')R_i(-mx'', -my'')], \quad (5)$$

where ⊗ means convolution. The intensity of the coherent double-pass retinal image (short exposure) will be

$$I_i''(x'', y'') = |O_i''(x'', y'')|^2 = m^4|h_1(mx'', my'') \otimes [h_1(-mx'', -my'')R_i(-mx'', -my'')]|^2. \quad (6)$$

The incoherent double-pass image is obtained by averaging of the coherent images, as given by Eq. (6) (see Refs. 8 and 9 for further details on this averaging process). If the retinal reflection factor $[R_i(x'', y'')]$ is assumed to be a complex function with unit modulus and random phase, we find that the averaged double-pass image, $[I''(x'', y'')]$, is

$$\begin{aligned}\langle I\rangle = I''(x'', y'') &= \frac{1}{N}\sum_{i=1}^{N} I_i''(x'', y'')\\ &\propto |h_1(mx'', my'')|^2 \otimes |h_1(-mx'', -my'')|^2\\ &= P(mx'', my'') \otimes P(-mx'', -my''), \quad (7)\end{aligned}$$

where N is the number of short-exposure images that are averaged and $P(mx'', my'')$ is the PSF of the eye (single-pass retinal image of a point test). The double-pass retinal image is related to the PSF (single-pass retinal image) by the autoconvolution with a negative sign in the argument of one of the PSF's; this autoconvolution indeed is the autocorrelation of the PSF. The change of variable above Eq. (5) allowed us finally to obtain the usual form of the autocorrelation.

An intuitive explanation of this result is illustrated in Fig. 1. An off-axis point source O is subject to coma, resulting in the asymmetric (comalike) single-pass PSF shown in the retinal plane. The second-pass imaging process, which proceeds in reverse direction from right to left, produces an inverted geometrical image of the PSF, $[P(-mx'', -my'')]$, which is convolved with the PSF of the second pass $[P(mx'', my'')]$, which has the same orientation as in the first pass. The convolution of an image with a copy of itself, rotated 180 deg, is an autocorrelation that is always even symmetric.

The ocular MTF, $[M(u, v)]$, can be calculated from the double-pass image as

$$\begin{aligned}M(u, v) &= \{|\mathrm{FT}[I''(x'', y'')]|\}^{1/2}\\ &= \{|\mathrm{FT}[P(mx'', my'') \otimes P(-mx'', -my'')]|\}^{1/2}\\ &= \{|\mathrm{FT}[P(mx'', my'')]\mathrm{FT}[P(-mx'', -my'')]|\}^{1/2}\\ &= [|H(u, v)H(-u, -v)|]^{1/2}\\ &= [H(u, v)H^*(u, v)]^{1/2}, \quad (8)\end{aligned}$$

where $H(u, v) = \mathrm{FT}[P(mx'', my'')] = M(u, v)\exp[iO_f(u, v)]$ is the optical transfer function; u, v are the spatial-frequency coordinates, and FT means Fourier transformation. The phase $O_f(u, v)$ is the phase transfer function (PTF), and when it is computed from the double-pass image $I''(x'', y'')$ it is a constant. The reason is that the Fourier transform of a real and even function [as is the aerial image, $I''(x'', y'')$, according to relation (7)] is also a real and even function.[20] Previous practitioners of

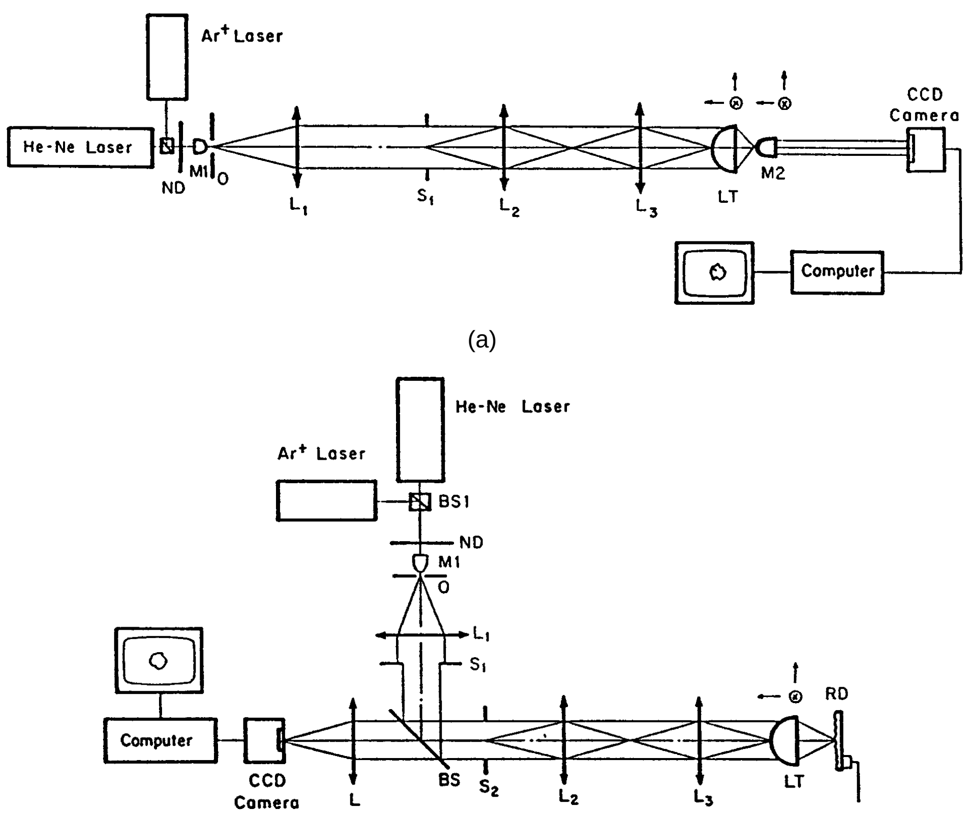

Fig. 2. Experimental setups for recording the (a) single-pass and (b) double-pass PSF's in an artificial eye, LT. ND, neutral-density filter; M1, M2, microscope objectives (10×); O, 10-μm pinhole (object test); L1, collimator lens; L_2, L_3, Badal system lenses ($f' = 120$ mm); L, lens ($f' = 200$ mm); RD, rotating diffuser.

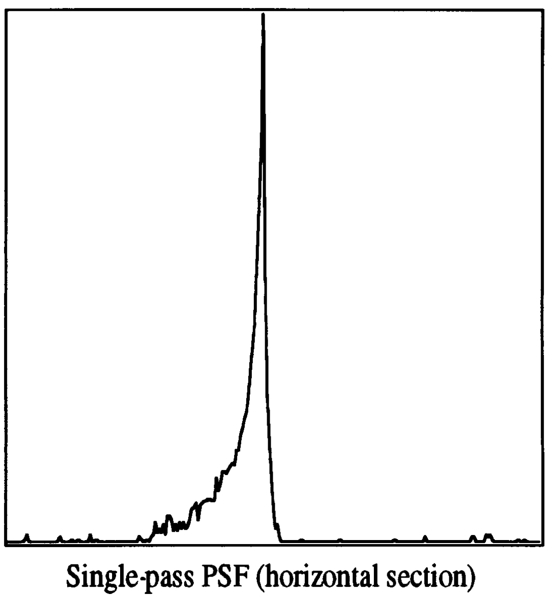

Fig. 3. Logarithm of the single-pass PSF $[P(x', y')]$ in a gray-level image and a 1-D horizontal section.

the double-pass method, including ourselves,[8,21] assumed that the double-pass image was the autoconvolution of the retinal image (PSF), instead of the autocorrelation of the PSF, as has been shown here. Under that assumption, both the PTF and comalike aberrations could be obtained from the double-pass image.

B. Single- and Double-Pass Point-Spread Functions Measured in an Artificial Eye

To establish the validity of the above theory, we measured the single- and double-pass PSF's in an artificial eye. We chose an artificial eye because this permits access to the single-pass PSF as well as to the double-pass aerial image, whereas in the living eye, only the double-pass image is accessible. Figure 2 shows the two setups that we used. Figure 2(a) shows the setup for measuring the single-pass PSF. A Badal system, L_2-L_3, projected a 5-mm aperture, S_1, onto a 70-D lens, LT, which acted as the artificial eye. To measure the single-pass PSF with the required resolution, a 10× objective microscope, M_1, magnified the image of the object, O, on the CCD camera (HPC-1, Spectrasource Inc.) containing a full-frame CCD array (Tektronik TK1024CF, 1024 × 1024 pixels). Figure 2(b) shows the setup for measuring the double-pass image. Lens LT forms the image of the object, O, on a rotating diffuser, RD, placed in its focal plane. The function of the diffuser is to mimic the effect of eye movements, which render the light incoherent in the averaged double-pass image obtained in the real eye. The light is reflected back from the diffuser and after it has passed through the beam splitter, BS, another lens, L ($f' = 200$ mm), forms the double-pass PSF on the CCD camera. Both images are recorded and stored in an image-processing system as 256 × 256 pixels with 16 bits/pixel images, under the same conditions of focus, pupil size, and centering.

We have chosen as an example the results with a PSF that suffers from coma. To produce coma, we displaced the incident beam horizontally with respect to the center of lens LT, which is a situation equivalent to that

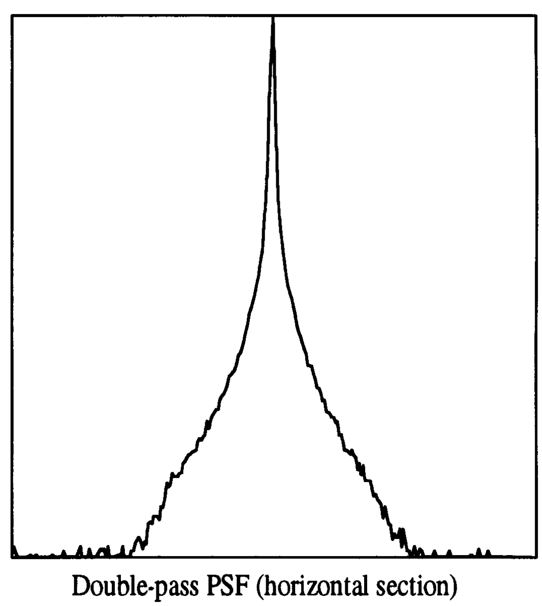

Fig. 4. Logarithm of the single-pass (aerial) image $[I''(x'', y'')]$: gray-level image and 1-D horizontal section.

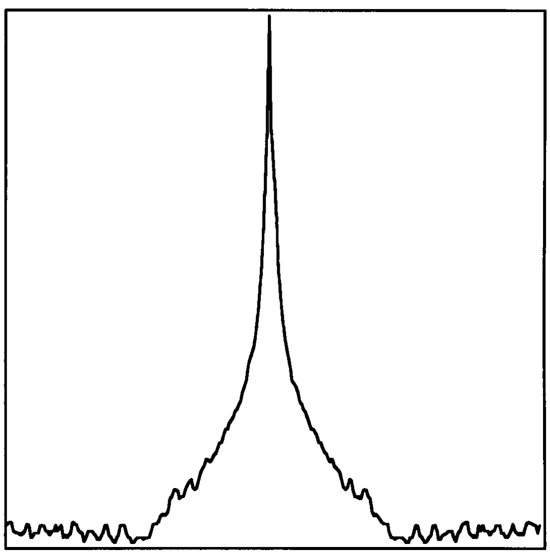

Autocorrelation of the single-pass PSF (horizontal section)

Fig. 5. Logarithm of the autocorrelation of the single-pass PSF: gray-level image and 1-D horizontal section.

of Fig. 1. To permit better visualization, because of the high dynamic range of the images, we present the logarithm of the resulting images in Figs. 3 and 4. Figure 3 shows the coma-shaped single-pass PSF $[P(mx'', my')]$ in a gray-level image and a one-dimensional (1-D) horizontal section. Figure 4 shows the double-pass PSF $[I''(x'', y'')]$ (gray-level image and 1-D horizontal section). From the single-pass PSF, the double-pass images were computed both by autocorrelation [according to relation (7)] and by autoconvolution. The logarithm of these computed double-pass images is presented in Figs. 5 and 6, respectively, in gray-level images and 1-D horizontal sections. These results should be compared with the measured double-pass image. The double-pass image observed experimentally (Fig. 4) is even symmetric, agreeing with the autocorrelation (Fig. 5) rather than with the autoconvolution (Fig. 6) of the single-pass PSF.

Figure 7 shows 1-D sections of the MTF's computed from the single-pass (dotted curve) and double-pass (solid curve) images. The two MTF's are quite similar, which shows that the MTF can be estimated accurately from the double-pass image, even though the aerial image has lost the asymmetry produced by coma.

C. Lateral Chromatic Aberration and the Double Pass

We also recorded single and double pass by using a He–Ne laser ($\lambda = 632$ nm) and one Ar^+ laser ($\lambda = 488$ nm). The setups of Fig. 2 allow us to record the images of both points simultaneously. Lens LT was twisted with respect to the incident beam to have a large, and then more easily measurable, lateral or transverse chromatic aberration. Figures 8(a) and 8(b) show the single- and double-pass PSF's, respectively, for red and blue sources. Taking into account the appropriate numbers for the magnification in both configurations, we found a separation between the peaks of the red and the blue images in the single pass near 78 μm, whereas in the double-pass images this distance was near 9 μm. These measurements indicate that the lateral chromatic aberration is nearly completely compensated in the second pass. This experiment confirms that the double-pass technique

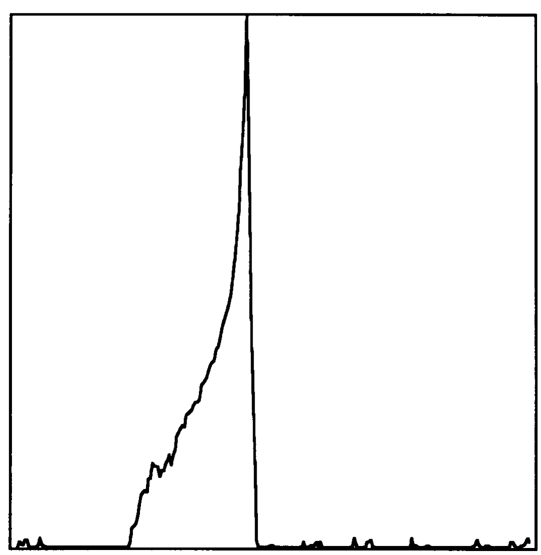

Autoconvolution of the single pass PSF (horizontal section)

Fig. 6. Logarithm of the autoconvolution of the single-pass PSF: gray-level image and 1-D horizontal section.

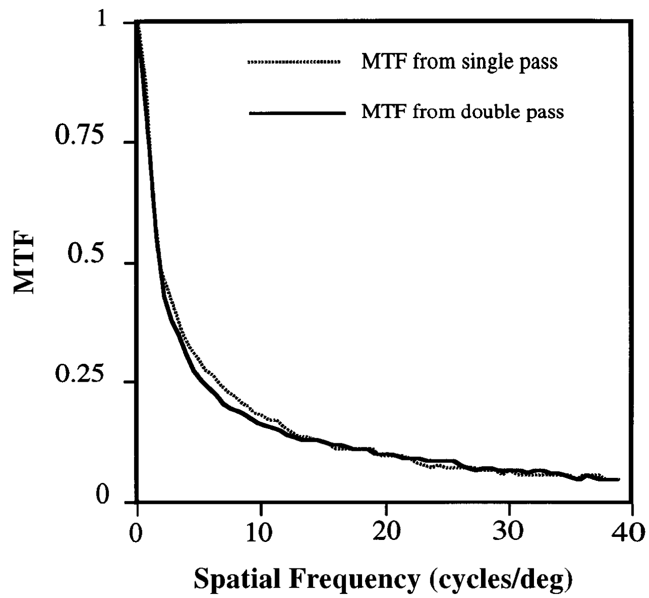

Fig. 7. 1-D sections of the MTF's computed from the single-pass PSF (solid curve) and from the double-pass image (dotted curve).

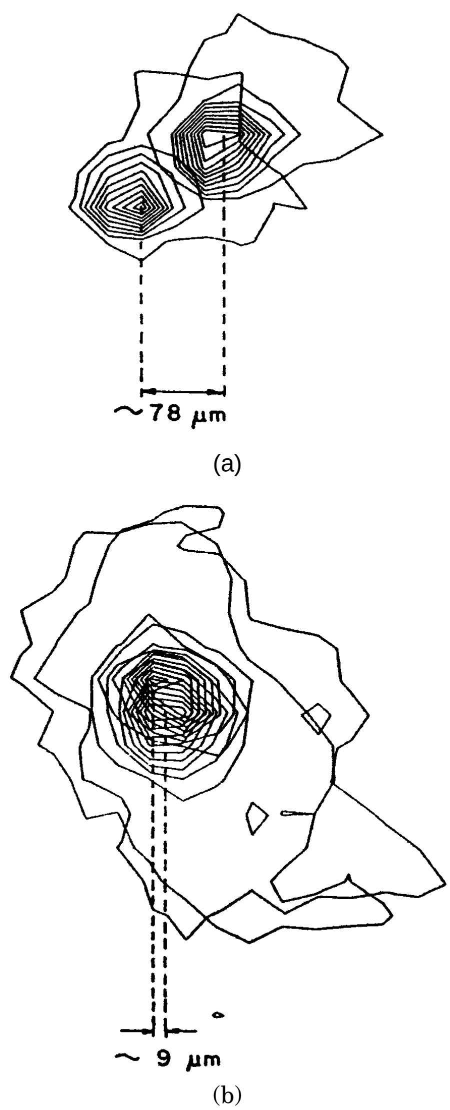

Fig. 8. (a) Single-pass PSF's and (b) double-pass images for red (632-nm) and blue (488-nm) light.

is not appropriate for determining lateral chromatic aberration in the human eye.

3. DISCUSSION

The image-formation process that removes asymmetries, caused by odd monochromatic aberrations, from the double-pass aerial image has a similar influence on chromatic aberrations that generate asymmetric single-pass PSF's. Indeed, any aberration that produces asymmetry in the single-pass PSF, such as distortion as well as coma and lateral chromatic aberration, will appear as even-symmetric blurring in the double-pass aerial image. Consequently, the actual retinal PSF cannot be easily determined from double-pass measurements, because the double-pass image is related to the single-pass (retinal) image through autocorrelation instead of autoconvolution, as was previously assumed by theorists and practitioners[2,8] of the double-pass method. All the phase information is lost in the double-pass images. This implies that previous PTF determinations from the double pass[21] were not correct. They clearly underestimated the resulting PTF by the assumption that the double-pass image was the autoconvolution of the retinal image. This fact can explain the discrepancies among some subjective methods that found important amounts of coma and large values of the phase transfer, whereas no double-pass studies have found coma either in the fovea or in the periphery. A review of typical double-pass images shows that they always have approximately an even symmetry, corresponding to an image given by Eq. (8). Despite the prediction of the mathematical analysis, PTF's are slightly nonuniform and coma is small but not zero in the double pass. The reason could be that some spatial inhomogeneities in the retinal reflection or in the measuring beam introduce additional asymmetries. Here, it is interesting to see Fig. 4 of Ref. 21, in which the PSF obtained from the double pass and the PSF corresponding to a zero (or flat) PTF are compared. Only small differences appear, because the actual double-pass image was already symmetrized in the second pass.

Despite the limitations on the double-pass method described here, we have some evidence that the importance of comalike aberrations in the peripheral retina is limited. With the accommodation paralyzed, we recorded aerial images, looking for the horizontal and vertical astigmatic foci.[22] These results together with others from measurements with natural pupil and accommodation[10] showed that astigmatism, rather than coma, is the main aberration in the periphery. We found that once astigmatism is corrected with cylindrical lenses, the image quality of the eye declines very little with retinal eccentricity. Though coma does not produce an asymmetry in the double-pass aerial image, it should blur the image nonetheless, as we have confirmed with computer simulations. Because the residual blur seen when astigmatism is corrected is small, coma should be relatively less important. We emphasize that the double-pass method remains valuable for studying the eye's optical performance because the ocular MTF can be computed from the double-pass image. In the understanding of the relative contributions of optical and neural stages in the visual system, the MTF plays a prominent role.[23–25]

It may be possible to recover the phase information lost in the double passage through the eye with the use of phase-retrieval algorithms[26] that are widely used in other applications.[27] Alternatively, it may also be possible to modify the double-pass method, using different entrance and exit pupil diameters, to obtain complete information. In addition, subjective methods for measuring phase errors[16] or objective methods that measure the wave-front error in the pupil plane of the eye, such as the objective aberroscope method[28] or the Hartmann–Shack method,[29] allow the PTF to be measured.

ACKNOWLEDGMENTS

This research was supported by the Comisión Interministerial de Ciencia y Tecnología, Spain, under grant TIC910438, and by National Institutes of Health grants EY01319 and EY04367 to D. R. Williams. The authors thank D. G. Green for a critical revision of the manuscript.

REFERENCES

1. W. N. Charman, "Optics of the human eye," in *Visual Optics and Instrumentation,* Vol. 1 of *Vision and Visual Dysfunction,* J. R. Cronly-Dillion, ed. (Macmillan, London, 1991), pp. 1–26.
2. M. F. Flamant, "Étude de la repartition de lumière dans l'image retinienne d'une fente," Rev. Opt. **34,** 433–459 (1955).
3. J. Krauskpof, "Light distribution in human retinal images," J. Opt. Soc. Am. **52,** 1046–1050 (1962).
4. F. W. Campbell and R. W. Gubisch, "Optical image quality of the human eye," J. Physiol. (London) **186,** 558–578 (1966).
5. R. W. Gubisch, "Optical performance of the human eye," J. Opt. Soc. Am. **57,** 407–415 (1967).
6. R. Rohler, U. Miller, and M. Aberl, "Zur Messung der Modulatonsubertragungsfunktion des Lebenden menschlichen Auges in reflektierten Licht," Vision Res. **9,** 407–428 (1969).
7. J. A. M. Jennings and W. N. Charman, "Off-axis image quality in the human eye," Vision Res. **21,** 445–454 (1981).
8. J. Santamaría, P. Artal, and J. Bescós, "Determination of the point-spread function of human eyes using a hybrid optical–digital method," J. Opt. Soc. Am. A **4,** 1109–1114 (1987).
9. P. Artal and R. Navarro, "Simultaneous measurement of two-point-spread functions at different locations across the human fovea," Appl. Opt. **31,** 3646–3656 (1992).
10. R. Navarro, P. Artal, and D. R. Williams, "Modulation transfer of the human eye as a function of retinal eccentricity," J. Opt. Soc. Am. A **10,** 201–212 (1993).
11. J. G. van Blockland and D. van Norren, "Intensity and polarization of light scattered at small angles from the human fovea," Vision Res. **26,** 485–494 (1986).
12. J. M. Gorrand, "Reflection characteristics of the human fovea assessed by reflectomodulometry," Ophthalmol. Physiol. Opt. **9,** 53–60 (1989).
13. D. R. Williams, D. Brainard, M. MacHahon, and R. Navarro, "Double-pass and interferometric measures of the optical quality of the eye," J. Opt. Soc. Am. A (to be published).
14. J. F. Simon and P. Denieul, "Influence of the size of the test employed in measurements of modulation transfer function of the eye," J. Opt. Soc. Am. **63,** 894–896 (1973).
15. J. J. Vos, J. Walraven, and A. Meeteren, "Light profiles of the foveal images of a point test," Vision Res. **16,** 215–219 (1976).
16. H. C. Howland and B. Howland, "A subjective method for the measurement of monochromatic aberrations of the eye," J. Opt. Soc. Am. **67,** 1508–1518 (1977).
17. M. C. W. Campbell, E. M. Harrison, and P. Simonet, "Psychophysical measurements of the blur on the retina due to the optical aberrations of the eye," Vision Res. **30,** 1587–1602 (1990).
18. S. Marcos, P. Artal, and D. G. Green, "The effect of decentered small pupils on optical modulation transfer and contrast sensitivity," Invest. Ophthalmol. Vis. Sci. Suppl. **35,** 1258 (1994).
19. J. W. Goodman, *Introduction to Fourier Optics* (McGraw-Hill, New York, 1968).
20. R. Bracewell, *The Fourier Transform and Its Applications* (McGraw-Hill, New York, 1965).
21. P. Artal, J. Santamaría, and J. Bescós, "Phase-transfer function of the human eye and its influence on point-spread function and wave aberration," J. Opt. Soc. Am. A **5,** 1791–1795 (1988).
22. P. Artal, R. Navarro, D. H. Brainard, S. J. Galvin, and D. R. Williams, "Off-axis optical quality of the eye and retinal sampling," Invest. Ophthalmol. Vis. Sci. Suppl. **33,** 3241 (1992).
23. P. Artal, M. Ferro, I. Miranda, and R. Navarro, "Effects of aging in retinal image quality," J. Opt. Soc. Am. A **10,** 1656–1662 (1993).
24. M. A. Losada, R. Navarro, and J. Santamaría, "Relative contribution of optical and neural limitations to human contrast sensitivity at different luminance levels," Vision Res. **33,** 2321–2336 (1993).
25. N. Sekiguchi, D. R. Williams, and D. H. Brainard, "Efficiency in detection of isoluminant and isochomatic interference fringes," J. Opt. Soc. Am. A **10,** 2118–2133 (1993).
26. P. Artal, J. Santamaría, and J. Bescós, "Retrieval of wave aberration of human eyes from actual point-spread-function data," J. Opt. Soc. Am. A **5,** 1201–1206 (1988).
27. J. C. Dainty and J. R. Fienup, "Phase retrieval and image reconstruction for astronomy," in *Image Recovery: Theory and Applications,* H. Stark, ed. (Academic, New York, 1987), pp. 231–273.
28. G. Walsh, W. N. Charman, and H. C. Howland, "Objective technique for the determination of monochromatic aberrations of the human eye," J. Opt. Soc. Am. A **1,** 987–992 (1984).
29. J. Liang, B. Grimm, S. Goelz, and J. Bille, "Objective measurement of wave aberrations of the human eye with the use of a Hartmann–Shack wave-front sensor," J. Opt. Soc. Am. A **11,** 1949–1957 (1994).